Supplement of Atmos. Chem. Phys., 19, 9333–9350, 2019
https://doi.org/10.5194/acp-19-9333-2019-supplement

Atmospheric Chemistry and Physics
Open Access
EGU

Supplement of

Optimization of process models for determining volatility distribution and viscosity of organic aerosols from isothermal particle evaporation data

Olli-Pekka Tikkanen et al.

Correspondence to: Olli-Pekka Tikkanen (op.tikkanen@uef.fi)

Supplementary material

Table S1: Parameters of MCGA optimization. Columns from left to right are name of the data set, number of candidates in a population, number of elite candidates in a generation, number of generation and the number of candidates drawn in the MC part

Data set	$N_{population}$	N_{elite}	$N_{generation}$	N_{MC}
Artificial data set 1	600	30	10	5130
Artificial data set 2	600	30	10	5130
Artificial data set 3	600	30	10	5130
Artificial data set 4	600	30	10	5130
Mixture 1	600	30	10	5130
Mixture 2	600	30	10	5130
Mixture 3	400	20	10	3420
Mixture 4	400	20	10	3420

Table S2: The saturation concentrations and mole fractions of each evaporating compound at the start of the evaporation in the artificial data set 4

Compound #	C_{sat} (μgm^{-3})	x_{mole} (t=0s)	Compound #	C_{sat} ($\mu g\ m^{-3}$)	x_{mole} (t=0s)
1	$3.27 \cdot 10^{-5}$	0.053	21	$6.47 \cdot 10^{-1}$	0.025
2	$3.55 \cdot 10^{-5}$	0.053	22	1.67	0.022
3	$8.86 \cdot 10^{-5}$	0.050	23	1.80	0.022
4	$1.07 \cdot 10^{-4}$	0.050	24	5.73	0.018
5	$3.02 \cdot 10^{-4}$	0.047	25	6.25	0.018
6	$3.67 \cdot 10^{-4}$	0.046	26	7.28	0.018
7	$4.38 \cdot 10^{-4}$	0.046	27	13.72	0.016
8	$5.45 \cdot 10^{-4}$	0.045	28	37.07	0.013
9	$6.09 \cdot 10^{-4}$	0.045	29	59.29	0.011
10	$6.04 \cdot 10^{-3}$	0.038	30	89.93	0.010
11	$8.73 \cdot 10^{-3}$	0.037	31	99.71	0.010
12	$8.85 \cdot 10^{-3}$	0.037	32	114.89	0.010
13	$2.67 \cdot 10^{-2}$	0.034	33	225.40	0.008
14	$3.24 \cdot 10^{-2}$	0.033	34	239.17	0.008
15	$1.16 \cdot 10^{-1}$	0.029	35	254.60	0.007
16	$2.78 \cdot 10^{-1}$	0.027	36	260.78	0.007
17	$3.05 \cdot 10^{-1}$	0.027	37	698.02	0.004
18	$4.04 \cdot 10^{-1}$	0.026	38	1380.27	0.002
19	$5.62 \cdot 10^{-1}$	0.025	39	2104.00	0.001
20	$5.96 \cdot 10^{-1}$	0.025	40	3059.89	0.001

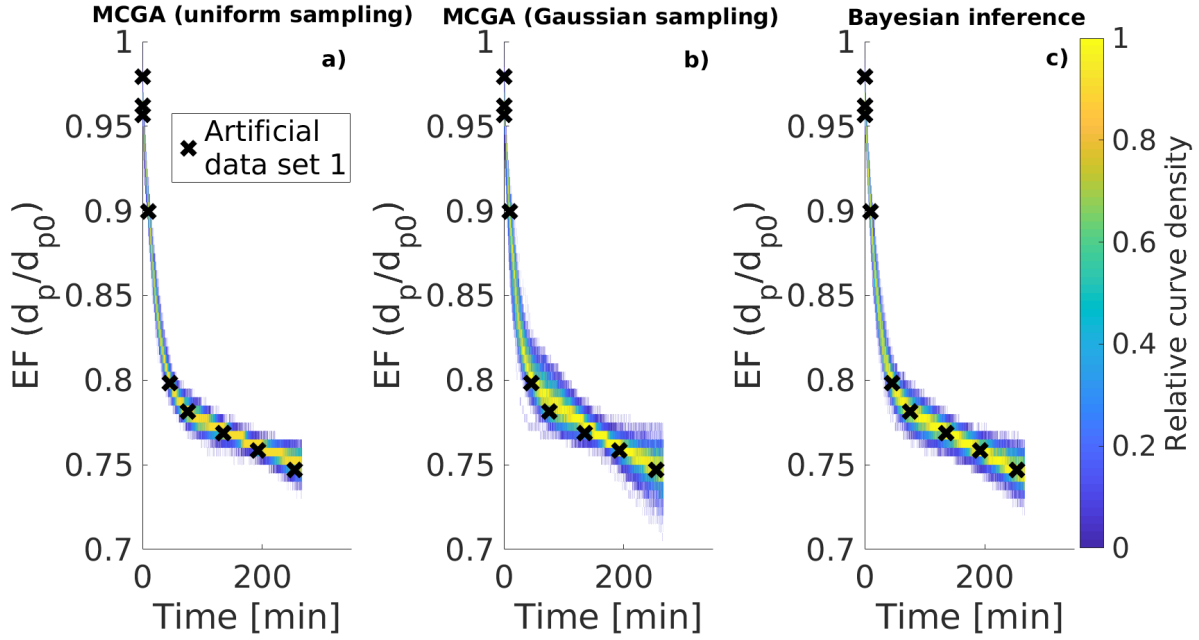

Figure S1: Relative evaporation curve density of the three different optimization schemes applied to artificial data set 1. The relative evaporation curve density is calculated by dividing the EF and time space to grids and counting how many of the simulated evaporation curve goes through a particular grid box. The counts are then normalized by the highest count in every time column. White color indicates that no simulation goes through that area. a) MCGA method with uniform sampling of the parameter space. b) MCGA with sampling similar to the Bayesian inversion method (see main text, Sect. 3)
c) Bayesian inference method.

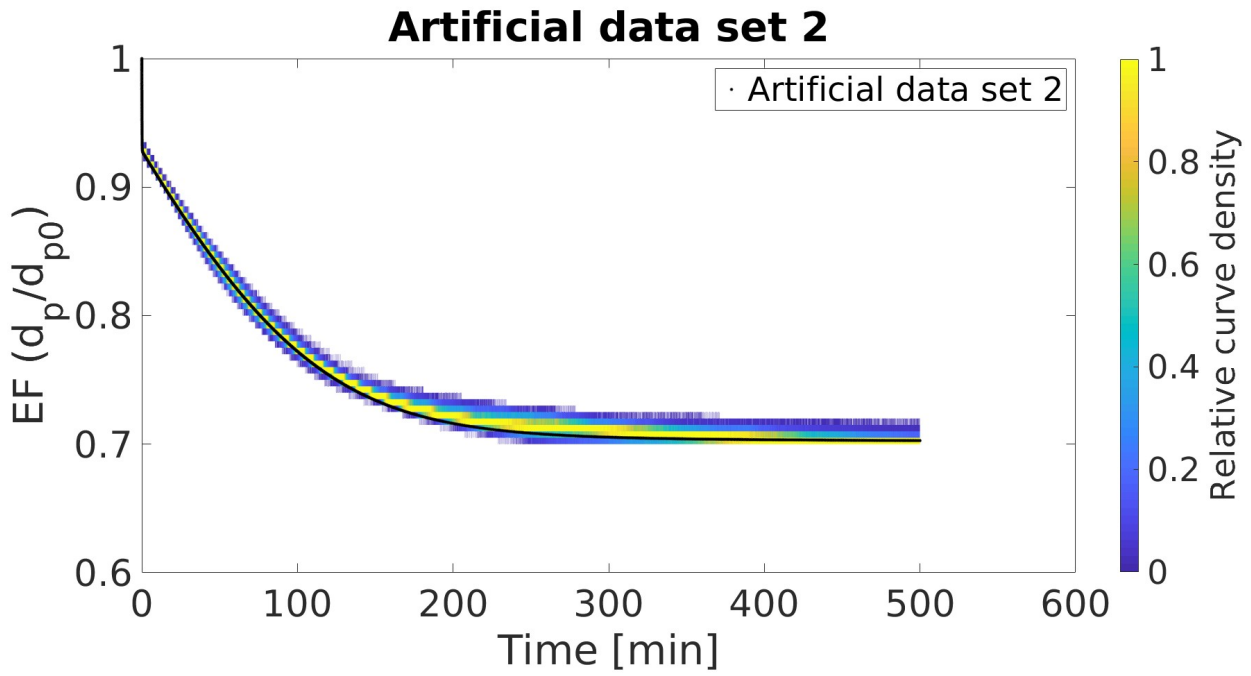

Figure S2: Relative evaporation curve density of the 500 MCGA optimization rounds for the artificial data set 2.

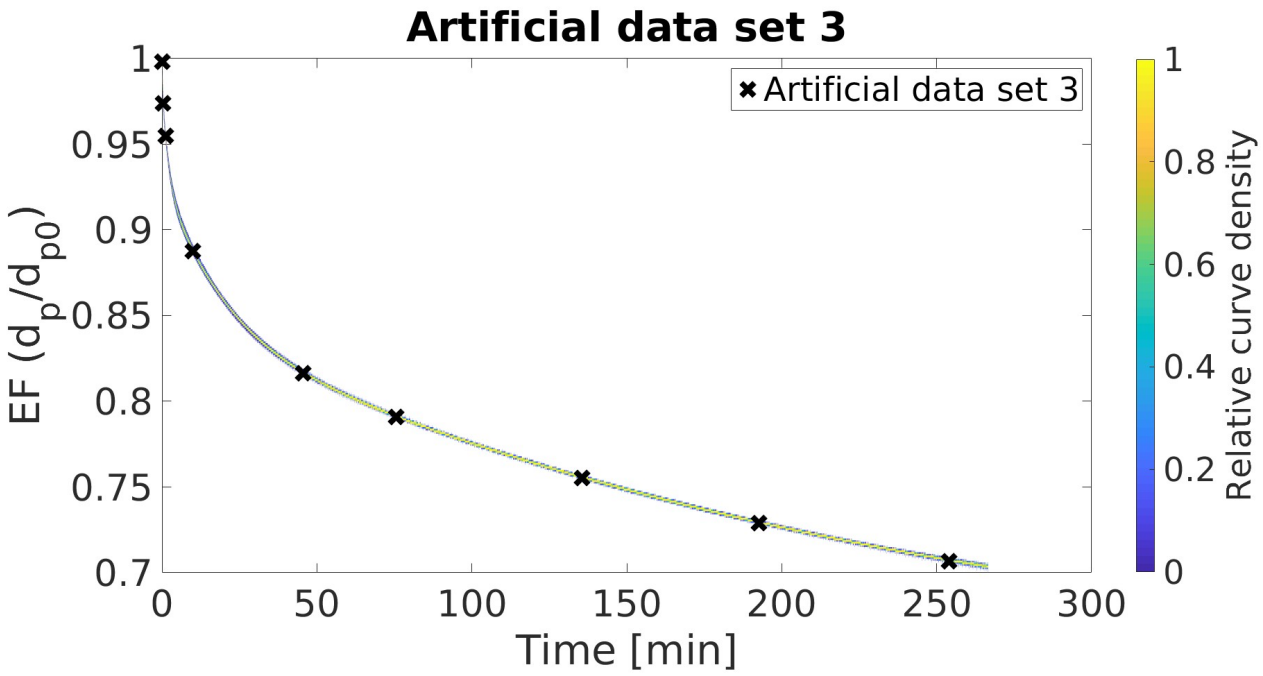

Figure S3: Relative evaporation curve density of the 500 MCGA optimization rounds for the artificial data set 3.

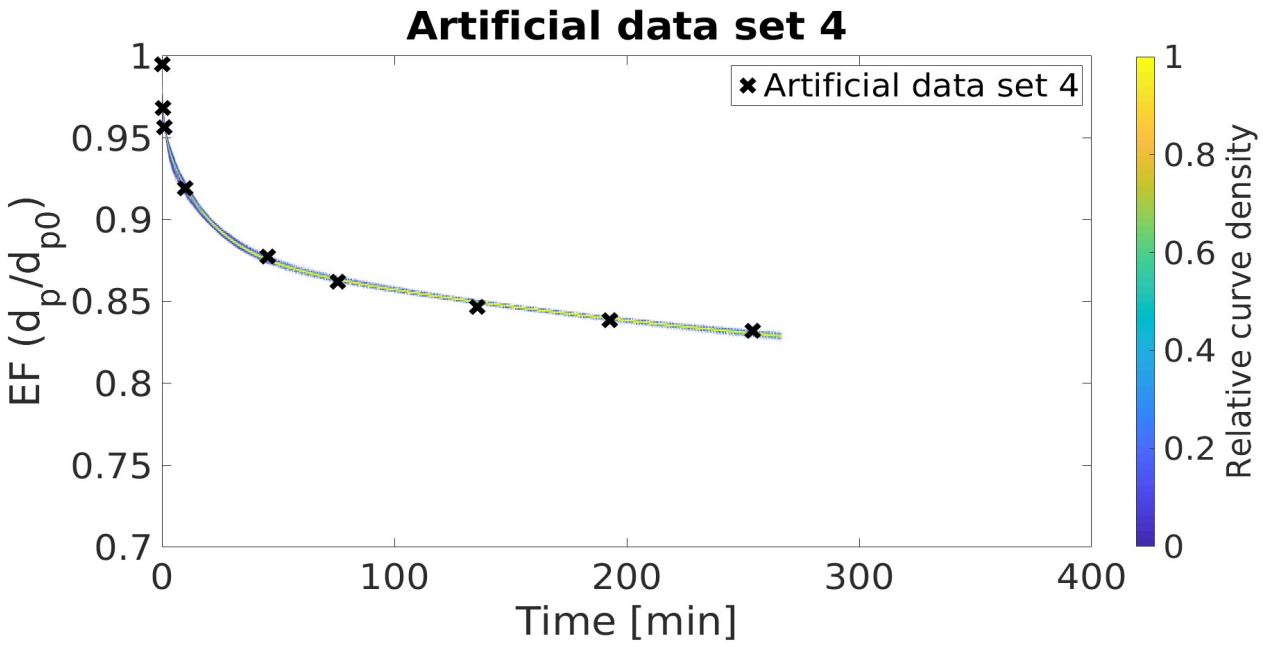

Figure S4: Relative evaporation curve density of the 500 MCGA optimization rounds for the artificial data set 4.

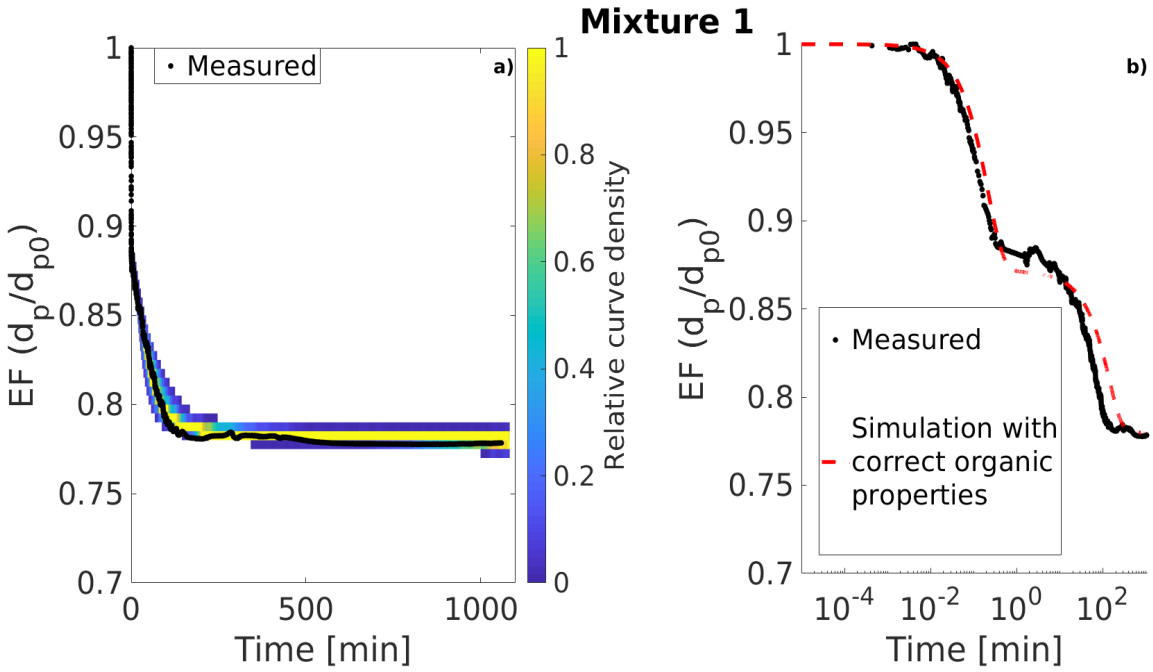

Figure S5: a) Relative evaporation curve density of the 100 MCGA optimization rounds from the optimization of the LLEVAP model to match measured particle evaporation of particles generated from mixture 1. b) Measured evaporation (black dots) and modelled evaporation (red dashed line) calculated by using correct properties of mixture 1 as an input.

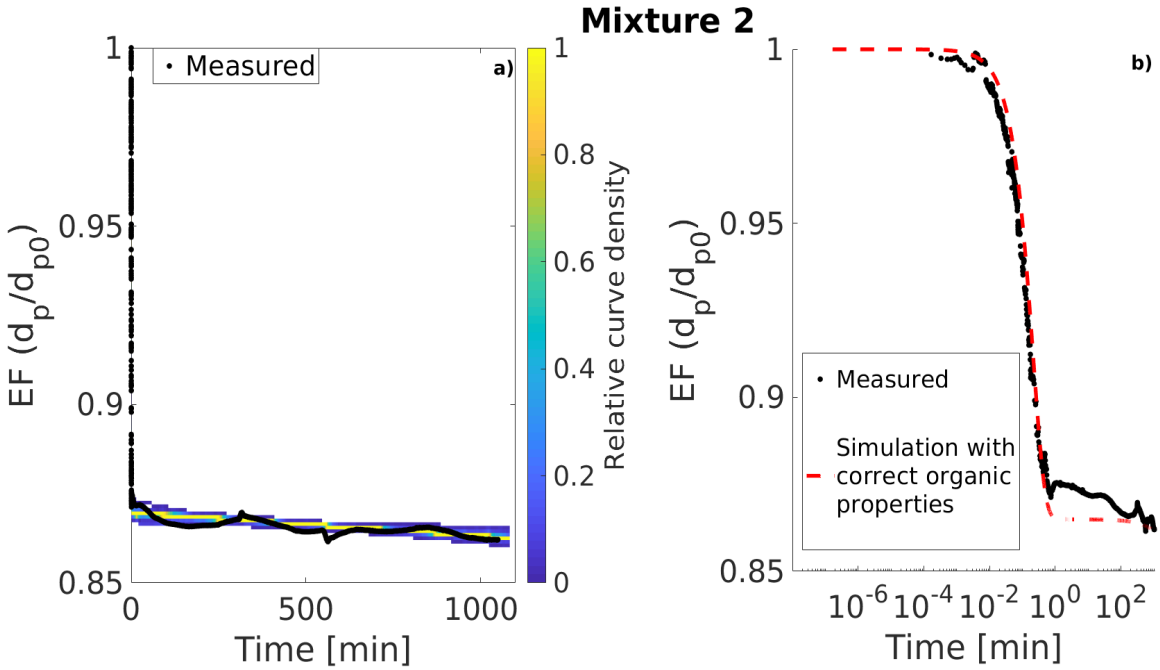

Figure S6: a) Relative evaporation curve density of the 100 MCGA optimization rounds from the optimization of the LLEVAP model to match measured particle evaporation of particles generated from mixture 2. b) Measured evaporation (black dots) and modelled evaporation (red dashed line) calculated by using correct properties of mixture 2 as an input.

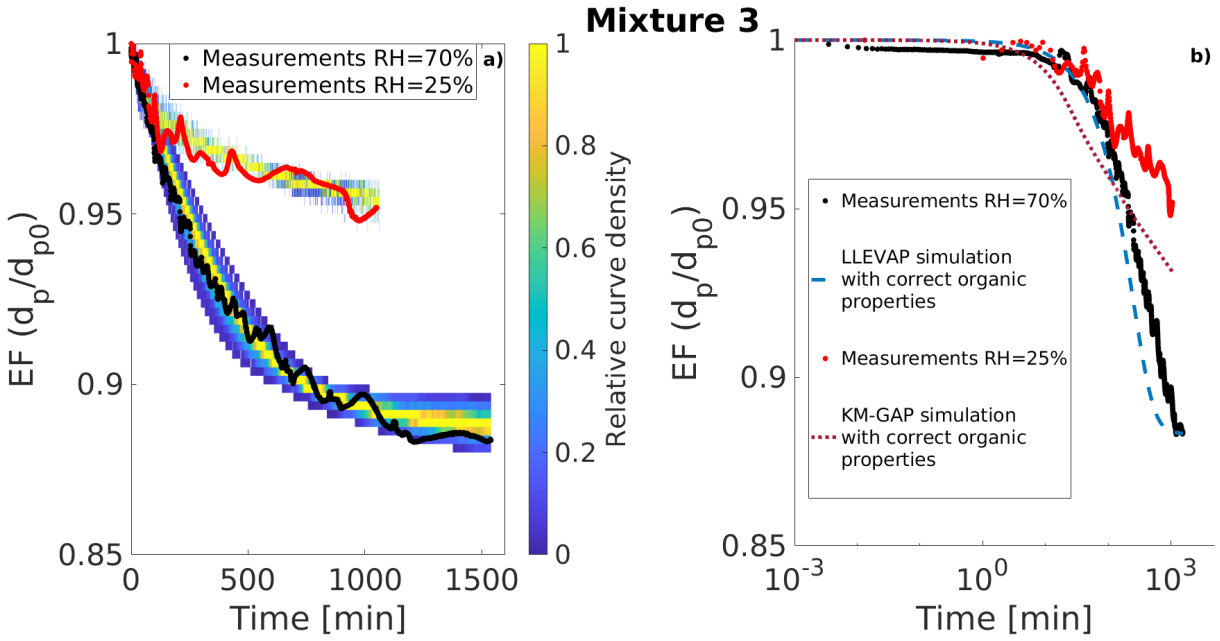

Figure S7: a) Relative evaporation curve density of the 100 MCGA optimization rounds from the optimization of the LLEVAP model to match measured particle evaporation at high RH (black dots) and KM-GAP model to match measured evaporation at lower RH (red dots). The particles, whose evaporation was measured, were generated from mixture 3. b) Measured evaporation (black dots for high RH and red dots for low RH) and modelled evaporation (red and brown dashed line) calculated by using correct properties of mixture 3 as an input.

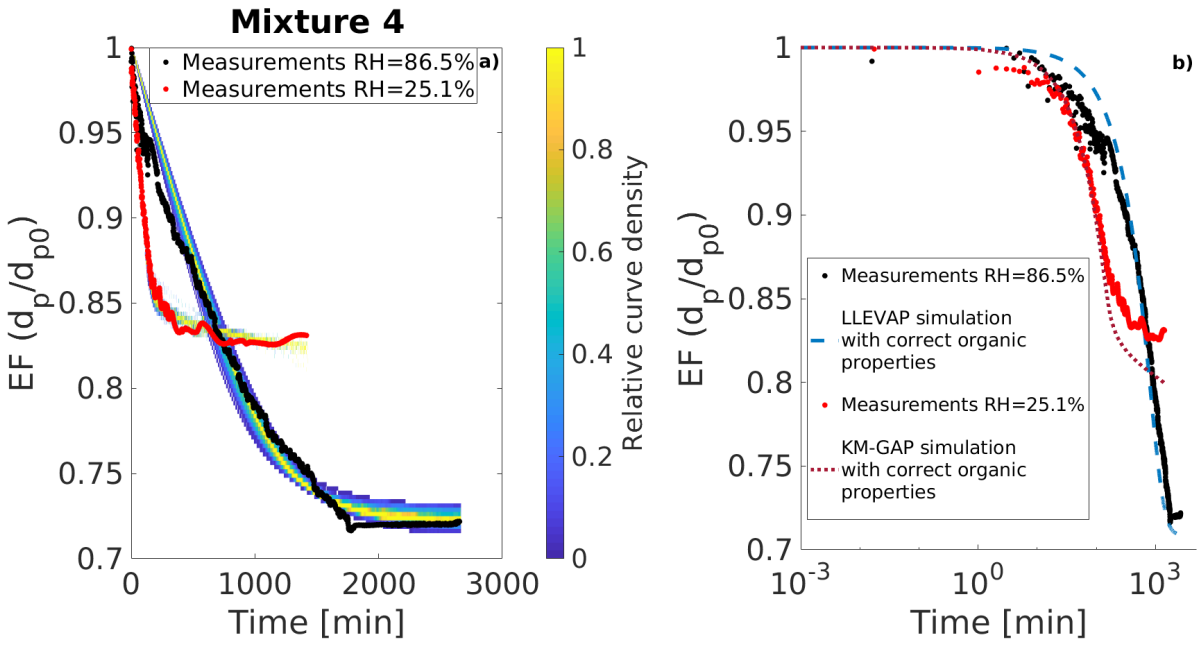

Figure S8: a) Relative evaporation curve density of the 100 MCGA optimization rounds from the optimization of the LLEVAP model to match measured particle evaporation at high RH (black dots) and KM-GAP model to match measured evaporation at lower RH (red dots). The particles, whose evaporation was measured, were generated from mixture 4. b) Measured evaporation (black dots for high RH and red dots for low RH) and modelled evaporation (red and brown dashed line) calculated by using correct properties of mixture 4 as an input.

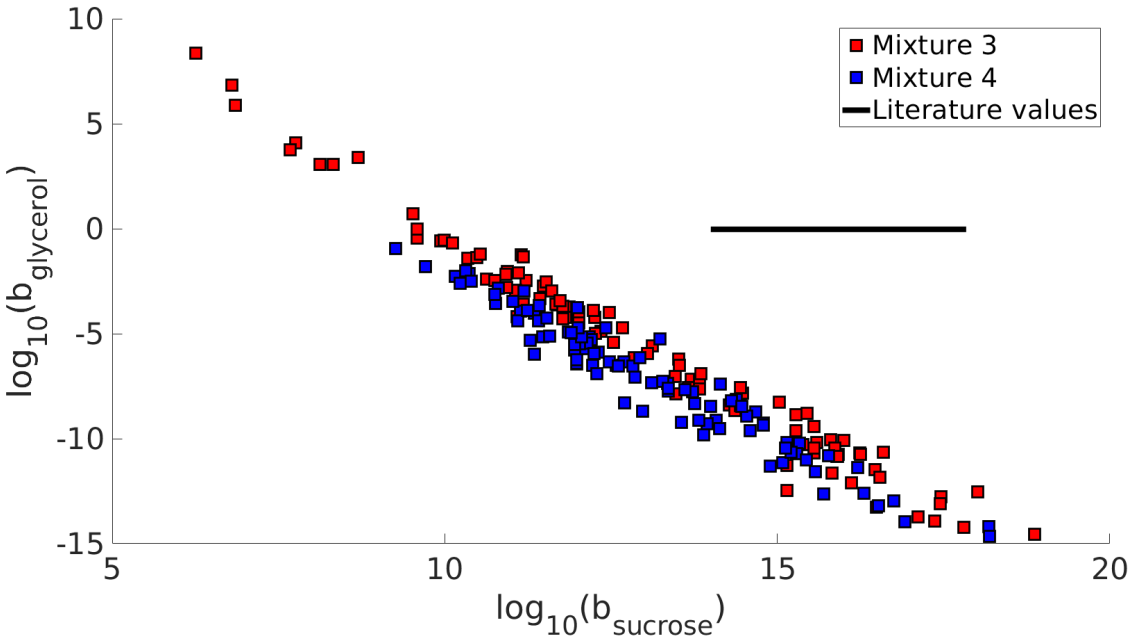

Figure S9: The correlation of estimated *b*-parameters for sucrose and glycerol in mixtures 3 and 4. The black line shows the range of literature values.